

Self-balancing Two-wheel Electric Vehicle (STEVE)

Abdelkareem M. Muhtaseb, Mohsen H. Shawar, Karim A. Tahboub
Mechanical Engineering Department
Palestine Polytechnic University
Hebron, Palestine

Abstract—STEVE is an applied research project to design, analyze, and construct an electric vehicle with two parallel wheels similar to Segway. A rider holds the steering while standing. The vehicle through an onboard-control system is balancing itself as well as responds to commands implied by the movement of the rider. For example, if the rider leans forward, the vehicle will accelerate in the forward direction and vice versa. Accelerometer and gyrometer are used to make tilt angle estimation. The estimation of the tilt angle is done using Kalman filter. Also, this vehicle can also turn to the right and to the left as commanded by the rider. Overall, this vehicle can move quickly over a long distance with only one battery charge.

Keywords—Segway; Embedded control; Kalman filter; Self-balancing; Modeling

I. INTRODUCTION

This paper represents STEVE as an applied research project. The mechatronics system is followed in this work. The first section of this paper makes an introduction. The second section introduces an overview of STEVE. The electrical design of STEVE is discussed in the third section. The modeling of STEVE is presented in the fourth section. The fifth section of this paper talks about STEVE control system and orientation estimation. The simulation and experimental results are presented in the sixth and seventh section respectively.

A. Concept of the project

In 2001 a new form of transportation was unveiled. Inventor Dean Kamen unveiled the Segway [1]. It has a standing platform between two coaxial wheels with handlebar protruding up from it. The rider of the Segway can ride it by leaning forwards to ride forward and leaning back to ride backwards [1]. Gyrometer and accelerometer sensors detect when the Segway is unbalanced and a computer drives the electric motors to balance the vehicle again or to ride forwards or backwards. The Self-balancing Two-wheel Electric Vehicle (STEVE) works in the same manner as with Segway. But for STEVE it is a main focus to be easy manufactured. In addition, STEVE allows for a person of average height and weight to safely ride it and also it is aesthetically pleasing.

B. Recognition of need

This project targets industrial, service, and all domestic sectors. It offers fast travelling speed in addition to personal comfort. This vehicle can be used by any individual working in an organization, company, or any public sectors. This vehicle can also be used in health and tourism sectors. For example,

people carrying Parkinson's disease (which slower the movement of a person) can use this vehicle in order to speed up his daily life activities. In tourism, this vehicle can be used for transportation in wide open regions reducing time of transportation. Tourists can see more and travel more using this vehicle and stay comfortable at the same time.

C. Project objectives

The main goal of this project is to design, and implement the vehicle to transport its rider from one place to another. This primary goal comprises inherently some other aims. For example, the studying of the concept and the problems related to vehicles which have two wheels similar to Segway. Also, the development of an accurate mathematical model of the system and convert it into a state space model. In addition, the obtaining of an electromechanical platform for performing experiments related to estimation of the tilt of bodies in space by employing gyrometer and accelerometer sensors.

II. OVERVIEW OF STEVE

A. Conceptual design

The main focus of the design of STEVE is to be easy manufactured, simple and aesthetically pleasing. So the conceptual design of STEVE consists of two main parts the mechanical components and the electrical components. The mechanical components are two coaxial wheels connected with two gearbox and motor assemblies, and these assemblies are connected with a platform that has an adjustable handlebar protruding up from it. The platform design is simple and has an enough space for the rider to stand up on it. One motor is not enough for the system since when the rider wants to rotate the speed of one wheel increases and the other wheel speed decreases. Because of that the system needs two motors.

The electrical components of the conceptual design of STEVE consist of two batteries fixed in front of the two motors on the platform. And these two batteries are connected to the power distribution circuit of STEVE in order to supply the electrical circuits with the needed power. These electrical circuits contain STEVE main control board, the power distribution circuit and STEVE Kalman filter board. The power distribution circuit is connected to STEVE main controller board and to STEVE Kalman filter board where gyrometer and accelerometer is connected. Gyrometer and accelerometer sensors are used to measure the tilt angle of STEVE in order to ensure the stability of the system. The controller of this system is implemented on microcontroller. The conceptual design of STEVE is shown in figure 1.



Figure 1. Conceptual design of STEVE.

B. Basic component selection

STEVE components are selected to be as follows:

- The mechanical components:
 - Motors and gearbox: 24V, 350W and 120rpm motors with gearbox are selected.
 - Platform: The platform is $55 \times 38 \times 1$ cm aluminum alloy.
 - Handlebar: The handlebar is made from steel tube that has a thickness of 1mm.
 - Wheels: Two wheels with 32cm radius are chosen for the vehicle.
- The electrical components:
 - Batteries: Two lead-acid 12V/12AH batteries are used.
 - Power distribution circuit: A power distribution circuit with output 5V and 15V is built.
 - Accelerometer: ADXL335 accelerometer is selected.
 - Gyrometer: MLX90609 gyrometer is chosen.
- Information and software:
 - Microcontroller: Two PIC18F4550 microcontrollers are used; one for the Kalman filter and the other is for the PD controller.
 - Motor drivers: Two power MOSFET circuits that can withstand a 24V, 20A, DC load are built to drive the motors of the system.

C. Implementation of STEVE

Figure 2 illustrates the schematic diagram of STEVE and it shows how the different components are related together.

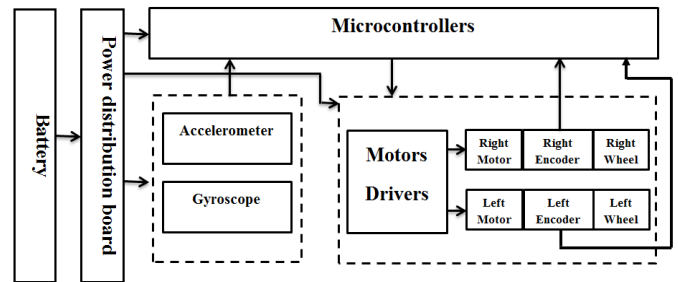


Figure 2. Schematic diagram of different components related together in STEVE.

III. ELECTRICAL DESIGN

The component space in this vehicle is very small, so electrical boards must be as small as possible. Because of that an electrical board that can achieve multitasks is designed and built for this vehicle. Figure 3 shows the STEVE main control board. This board is consisting of many regions as shown in the figure. Every region has a specific task that can achieve. The red region is the power distribution circuit region which is used to distribute power needed for STEVE components with different ranges of voltages as mentioned before. The green region is the main control unit of STEVE which consists of a microcontroller that contains the main control algorithm of the system. This region controls and manages the parts of the system. The yellow and blue regions are the first and second motors controllers. These regions get their commands from the main microcontroller in order to control the speeds of the two motors and get the encoders feedback from them.

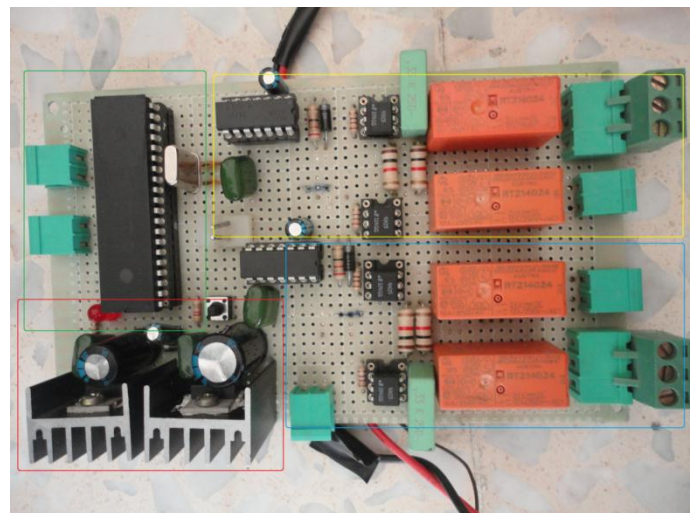


Figure 3. STEVE main control board.

IV. MODELING

A. Introduction

The dynamic performance of physical systems is obtained by utilizing the physical laws of mechanical, electrical, fluid and thermodynamic systems [2]. In general physical systems

are modeled with nonlinear differential equations with constant or variable coefficients.

Mathematical modeling of STEVE system tends to represent all important features of the system and describe its behavior in terms of differential equations. The needed model accuracy (closeness to the actual system) depends on the purpose [2]. Generally, a simplified model is needed to study the main characteristics of the system.

A basic model is derived for STEVE system which is simple and linear model for controller design and analysis purposes as accurately as possible. In the case of STEVE system, the following assumptions are used in deriving the mathematical model:

- There is point contact between the wheel and the ground not an area contact.
- There is no relative motion between platform and feet. So, the feet and the platform are always in contact.
- There is no slipping between the two wheels and the ground, this assumption means $x=R\theta$, in which θ is the angle of wheel rotation, and R is radius of wheel.
- The air resistance effects on the person, the platform and the wheels, are negligible.
- The oscillation of the rider around the x-axis is negligible.
- There is no damping between the wheels and platform.
- There is no damping in the motors.

In order to obtain the mathematical model of STEVE, Newton's law of motion is used to derive the basic differential equations that govern system's dynamics. Table I shows the variables and the parameters of the system.

B. Mathematical model of STEVE on horizontal flat road without rotation

The free body diagram of STEVE on horizontal flat road without rotation is shown in figure 4. Three nonlinear differential equations are describing the system in this case. These equations are as follows:

$$\left(J_{h_{com}} + M_h L_h^2\right) \ddot{\alpha} + M_h L_h \ddot{x} \cos(\alpha) - M_h g L_h \sin(\alpha) + k_t \alpha - k_t \phi + D_t \dot{\alpha} - D_t \dot{\phi} = -T_d \quad (1)$$

$$\left(M_p L_p^2 + J_{p_{com}}\right) \ddot{\phi} - M_p L_p \ddot{x} \cos(\phi) + M_p g L_p \sin(\phi) - k_t \alpha + k_t \phi - D_t \dot{\alpha} + D_t \dot{\phi} = T_d - T \quad (2)$$

$$\left(\frac{J_{w_{com}}}{R^2} + M_p + M_h + M_w\right) \ddot{x} - M_p \ddot{\phi} L_p \cos(\phi) + M_h \ddot{\alpha} L_h \cos(\alpha) + M_p L_p \dot{\phi}^2 \sin(\phi) - M_h \dot{\alpha}^2 L_h \sin(\alpha) = \frac{T}{R} \quad (3)$$

TABLE I. VARIABLES AND PARAMETERS

Symbol	Variables and parameters	Unit
x	Straight forward position	[m]
ϕ	Absolute tilt angle of the platform	[rad]
θ_{RW}	Angular displacement of the right wheel	[rad]
θ_{LW}	Angular displacement of the left wheel	[rad]
α	Absolute tilt angle of the human body	[rad]
δ	Absolute yaw angle of the system	[rad]
M_h	Mass of the human body	[kg]
$J_{h_{z_{com}}}$	Moment of inertia of the human body about COM in z-direction	[kg.m ²]
$J_{h_{y_{com}}}$	Moment of inertia of the human body about COM in y-direction	[kg.m ²]
M_{RW}	Mass of the right wheel	[kg]
$J_{RW_{z_{com}}}$	Moment of inertia of the right wheel about COM in z-direction	[kg.m ²]
M_{LW}	Mass of the left wheel	[kg]
$J_{LW_{z_{com}}}$	Moment of inertia of the left wheel about COM in z-direction	[kg.m ²]
M_p	Mass of the platform and feet	[kg]
$J_{p_{z_{com}}}$	Moment of inertia of platform and feet about COM in z-direction	[kg.m ²]
$J_{p_{y_{com}}}$	Moment of inertia of platform and feet about COM in y-direction	[kg.m ²]
R_R	Right wheel Radius	[m]
R_L	Left wheel Radius	[m]
L_h	Distance between the z-axis and the center of mass of the human	[m]
L_w	Distance from the center point and the center of the wheel	[m]
L_f	Distance from the center point and the center of the ankle joint	[m]
g	Gravity constant	[m/s ²]
T_d	Input torque from the rider as a command for the vehicle [human produced torque]	[N.m]
T	Motors torque	[N.m]
L_p	Distance between the z-axis and the center of mass of platform	[m]
k_t	The ankle joint torsional stiffness	[N.m/rad]
D_t	The ankle joint torsional damping	[N.m.s/rad]

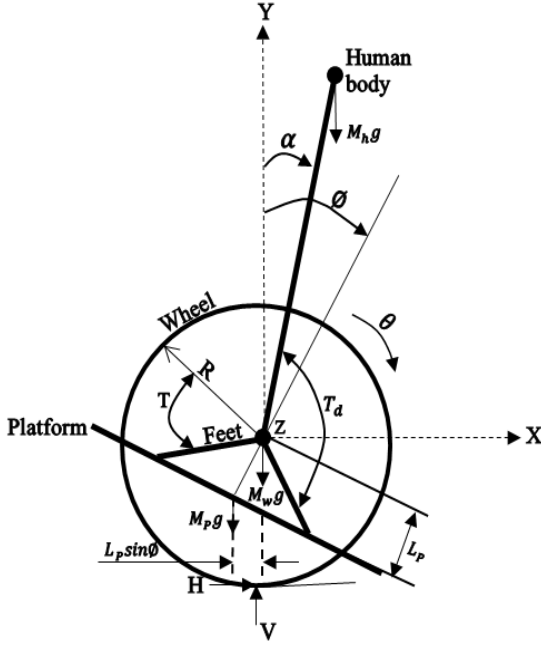


Figure 4. Free body diagram of STEVE on horizontal flat road without rotation.

C. Mathematical model of STEVE on horizontal flat road with rotation

The free body diagram of STEVE on horizontal flat road with rotation is shown in figure 5.

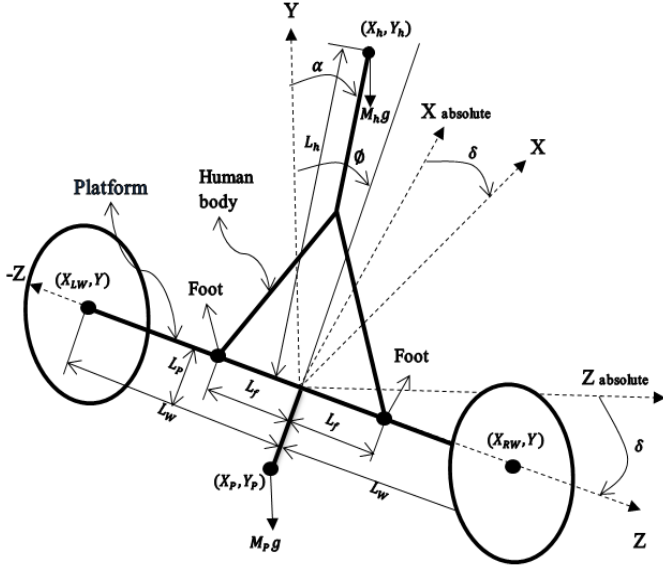


Figure 5. Free body diagram of STEVE on horizontal flat road with rotation.

Four nonlinear differential equations are describing the system in this case. These equations are as follows:

$$\begin{aligned} & \left(J_{h_{zcom}} + M_h L_h^2 \right) \ddot{\alpha} + M_h L_h \ddot{x} \cos(\alpha) - M_h L_h g + K_t \alpha - \\ & K_t \phi + D_t \dot{\alpha} - D_t \dot{\phi} = -T_d \end{aligned} \quad (4)$$

$$\begin{aligned} & \left(M_p L_p^2 + J_{P_{zcom}} \right) \ddot{\phi} - M_p L_p \ddot{x} \cos(\phi) + M_p L_p g \sin(\phi) - \\ & K_t \alpha + K_t \phi - D_t \dot{\alpha} + D_t \dot{\phi} = T_d - T \end{aligned} \quad (5)$$

$$\begin{aligned} & \left(\frac{J_{h_{ycom}}}{L_w} + \frac{J_{P_{ycom}}}{L_w} + \frac{L_w J_{Rw_{zcom}}}{R_R^2} + \frac{L_w J_{Lw_{zcom}}}{R_L^2} + L_w M_{Rw} + \right. \\ & \left. L_w M_{Lw} \right) \ddot{\delta} + \left(\frac{J_{Lw_{zcom}}}{R_L^2} - \frac{J_{Rw_{zcom}}}{R_R^2} + M_{Lw} - M_{Rw} \right) \ddot{x} = \\ & \left(\frac{R_R - R_L}{R_R R_L} \right) T + \left(\frac{R_R + R_L}{R_R R_L} \right) \Delta T \end{aligned} \quad (6)$$

$$\begin{aligned} & \left(M_h + M_p + M_{Rw} + M_{Lw} + \frac{J_{Rw_{zcom}}}{R_R^2} + \frac{J_{Lw_{zcom}}}{R_L^2} \right) \ddot{x} + \\ & \left(L_w M_{Lw} - L_w M_{Rw} + \frac{L_w J_{Lw_{zcom}}}{R_R^2} - \frac{L_w J_{Rw_{zcom}}}{R_L^2} \right) \ddot{\delta} - \\ & M_h L_h \dot{\alpha}^2 \sin(\alpha) + M_h L_h \ddot{\alpha} \cos(\alpha) + M_p L_p \dot{\phi}^2 \sin(\phi) - \\ & M_p L_p \ddot{\phi} \cos(\phi) = \left(\frac{R_R + R_L}{R_R R_L} \right) T + \left(\frac{R_R - R_L}{R_R R_L} \right) \Delta T \end{aligned} \quad (7)$$

D. Modeling summary

By comparing the equations that obtained from the mathematical model of STEVE on horizontal flat road without rotation with the equations that obtained from the mathematical model of STEVE on horizontal flat road with rotation, it can be seen that the first two equations are similar in the two cases. That is because the dynamics of the platform and the rider are the same in the two cases. But for the third equation in the first model it is separated into two equations in the second model. In order to make the two models become the same then assumptions must be made on the system.

If it is assumed that the two motors produces the same torque then (ΔT) will be equal to zero. Because of that it will be no rotation and that means (δ) will equal to zero. And since the two wheels have the same radius then the third equation parameters will be equal to zero and the equation will canceled. Also since (δ) became equal to zero then the fourth equation of the second model will be equal to the third one in the first model and that makes the two models became the same.

V. CONTROL AND ORIENTATION ESTIMATION

A. Control architecture

The understanding of the control architecture of the system is very important since it helps in designing the control system of the vehicle. Otherwise without understanding the control architecture then it will be very difficult to design a control system that can achieve the desired task of the system which is the transportation of the rider safely and comfortably.

Figure 6 shows the control architecture of STEVE. In this vehicle the rider gives STEVE two commands, the first one is a human produced torque, and the other one is the rotation command. The rider changing the tilt angle of the platform by applying a tilting torque on it, then the measurements of the sensors change. The accelerometer and gyrometer

measurements enter to the Kalman filter which makes an estimation of the tilting angle. After that, the controller starts to compensate the tilting angle by sending commands to the motors drivers in order to insure the stability of the rider. After the commands reach the motors drivers the motors starts to produce torques corresponding to the commands from the controller. That will cause the vehicle to accelerate.

The rider sends a rotation command to the vehicle by rotating a throttle fixed on the handlebar. Rotating the throttle causes a voltage change on its terminals. This change in voltage is measured by the analog to digital converter (ADC) in the microcontroller. Then the microcontroller sends a difference command to motors drivers which make one wheel rotating faster than the other. The encoders measure the angular displacements of the wheels in order to produce feedback for the rotation angle of the vehicle.

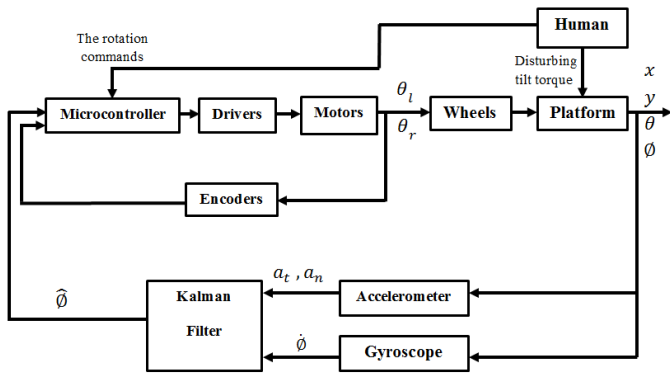


Figure 6. Block-diagram for the control architecture of STEVE.

Where:

a_t, a_n : are the tangential and normal acceleration on the rider and chassis.

$\hat{\theta}$: is the estimated tilt angle.

$\dot{\theta}$: is the tilting angular rate.

θ_l : is the angular displacement of the left wheel.

θ_r : is the angular displacement of the right wheel.

The system described in (section III) is an excellent test bed for control theories because it exhibits non-linear and unstable system. Control objectives for such systems are always challenging. Therefore, in this section, it is the aim to show how the system can be controlled using PD controller. The controller is designed utilizing the dynamics models developed in (section III).

The design of the mechanical structure of STEVE ensures that the ankle joints of the rider and the wheels axle to be at the same axis. This design increases the comfort of the rider and increases the stability of the system. In the case of no rider on the vehicle, the platform and the mechanical structure of STEVE will have a center of mass below the wheel axel. Then the system will behave as a simple pendulum and that makes it stable by its nature.

In the previous section it is assumed that there is no relative motion between the feet and the platform. Then the feet and the platform are modeled as one body. The input tilting commands come from the rider in the form of human produced torque " T_d ". This torque effects on the ankle joint.

Ankle joint has stiffness " K_t " and damping " D_t " that are not enough to stabilize the human inverted pendulum. Thus, a PD controller adds stiffness " K_p " and damping " K_d " to stabilize it and to give it good dynamic behavior. Farther, the human still exercise an extra torque " $T_{d_{eff}}$ " to cause a platform tilt. The human produced torque " T_d " and the human body controller are modeled in the design and simulation of the control system of STEVE. Figure 7 shows the simulation of the nonlinear model of STEVE on flat road with rotation. And the following equations is " T_d " equation.

$$T_d = T_{d_{eff}} + [K_p(\alpha - \alpha_d) + K_d(\dot{\alpha} - \dot{\alpha}_d)] + [K_t(\alpha - \phi) + D_t(\dot{\alpha} - \dot{\phi})] \quad (8)$$

Where $[K_p(\alpha - \alpha_d) + K_d(\dot{\alpha} - \dot{\alpha}_d)]$ is the human body controller, $[K_t(\alpha - \alpha_d) + D_t(\dot{\alpha} - \dot{\phi})]$ is the passive torque and α_d is the desired tilt angle of the human body which equal to zero.

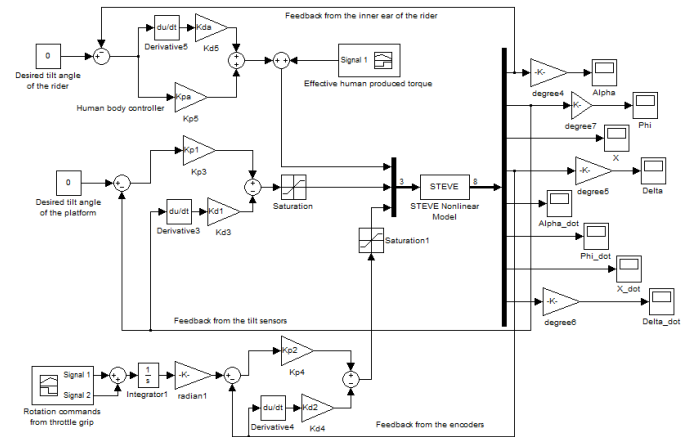


Figure 7. The simulation of the nonlinear model of STEVE on flat road with rotation.

B. Orientation estimation

The vehicle balances itself as well as responds to commands implied by the movement of the rider. For example, if the rider leans forward, the vehicle accelerates in the forward direction and vice versa. Because of that it is necessary for the controller to have the exact estimation of the tilt angle at every moment, and that to know the rider commands.

It is important to use both an accelerometer and a gyrometer combined with sensor fusion algorithms to give the controller an accurate estimate of the current system state [3]. The readings of the accelerometer and gyrometer are combined, such that the inaccuracies of each sensor will be compensated for by the other [4]. The accelerometer alone is unable to accurately measure the attitude of STEVE due to its

limited bandwidth. This means that it can only be accurate for slow variances in the tilt angle [4].

The accelerometer and gyrometer are fixed on the wheels axial line. One of the measuring axes of the accelerometer is in the radial direction and the other one is in the tangential direction. When the tilt angle of STEVE is changed then the effect of the gravity acceleration increases in one measuring axis of the accelerometer and decreases in the other axis and figure 8 shows this idea. The increasing and decreasing of the effect of the gravity acceleration is used to estimate the orientation angle. But the problem with using this method is that when the angular acceleration of rider and chassis is large so it produces large values of tangential and centrifugal acceleration. These accelerations will cause a large effect on the accelerometer signals. So it produces an inaccurate estimation of the tilt angle of STEVE.

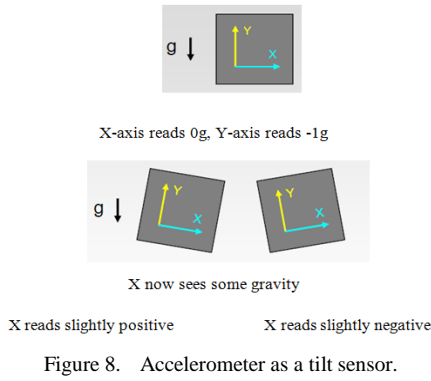


Figure 8. Accelerometer as a tilt sensor.

The gyrometer angle estimation is inaccurate at very low frequencies due to drift in the signal created by very low frequency noise in the angular rate measurement [4]. The signal from the gyrometer is fused with the accelerometer signal using Kalman filter in order to obtain accurate angle estimation. In other words, the accelerometer makes estimation of the tilt angle at low frequencies and the gyrometer makes estimation of the tilt angle at high frequencies. This presented a major challenge in this project to get an accurate estimation of the tilt angle. The Kalman filter dynamics and equations are as follows. Tahboub [5] state that:

The gyrometer generates a noisy angular acceleration signal that is internally integrated to yield the angular velocity superimposed with a drift such that:

$$\omega_c = \omega + \omega_{drift} + v_c \quad (T1)$$

Where ω is the actual angular velocity ($\omega = \dot{\varphi} = \dot{\alpha} + \dot{\theta}$), v_c is a Gaussian white measurement noise of variance δ_c , and ω_{drift} is the velocity drift that is assumed to be the integration of another Gaussian white noise v_{drift} of variance δ_{drift} as:

$$\dot{\omega}_{drift} = v_{drift} \quad (T2)$$

Notice that the low-frequency noise affecting the gyrometer's angular velocity is modeled here as an explicit drift signal. This representation aims at explicitly estimating the drift and thus canceling its effect on the estimation of angular velocity. On the other hand, the accelerometer generates acceleration signals contaminated with noise. Specifically in the tangential direction:

$$a_x = a + v_a \quad (T3)$$

Where a is the actual tangential acceleration (vertical to the body), v_a is a Gaussian white measurement noise of variance δ_a . The tangential acceleration has two components: the first is due to angular acceleration while the second is due to the tilt of the gravity vector:

$$a = \dot{\omega}h_a + g \sin\varphi \approx \dot{\omega}h_a + g\varphi \quad (T4)$$

Where h_a is the height of the accelerometer from the center of rotation. Thus Eq. (T3) becomes:

$$a_x = g\varphi + v_a \quad (T5)$$

Equations (T1) and (T5) represent the sensor dynamics of the system (in one dimension) whereas the process dynamics is given by:

$$\dot{\omega} = v_w \quad (T6)$$

$$\dot{\omega}_{drift} = v_{drift} \quad (T7)$$

In which $\dot{\omega}$ is considered to be solely generated by a Gaussian process white noise v_w of variance δ_w . The above equations can be collected together in state-space form as:

$$\begin{bmatrix} \dot{\varphi} \\ \dot{\omega} \\ \dot{\omega}_{drift} \end{bmatrix} = \begin{bmatrix} 0 & 1 & 0 \\ 0 & 0 & 0 \\ 0 & 0 & 0 \end{bmatrix} \begin{bmatrix} \varphi \\ \omega \\ \omega_{drift} \end{bmatrix} + \begin{bmatrix} 0 \\ v_w \\ v_{drift} \end{bmatrix} \quad (T8)$$

$$\begin{bmatrix} \omega_c \\ a_x \end{bmatrix} = \begin{bmatrix} 0 & 1 & 1 \\ g & 0 & 0 \end{bmatrix} \begin{bmatrix} \varphi \\ \omega \\ \omega_{drift} \end{bmatrix} + \begin{bmatrix} v_c \\ v_a \end{bmatrix} \quad (T9)$$

The state vector $x = [\varphi \ \omega \ \omega_{drift}]$ can be optimally estimated by a Kalman filter based on the two measurements $y = [\omega_c \ a_x]$ and given the process (w) and measurements (v) noise variances. In other words, the two measurements can be fused optimally to find the best possible estimates in the presence of process and measurement noise. The Kalman filter is realized by:

$$\hat{x} = F\hat{x} + L_{KF}(y - H\hat{x}) \quad (T10)$$

Where \hat{x} is the optimal estimate of x and L_{KF} is the static Kalman gain matrix that is obtained by solving the algebraic Riccati equation:

$$F.P + P.F^T + Q - P.H^T.R^{-1}.H.P = 0 \quad (T11)$$

And

$$L = P.H^T.R^{-1} \quad (T12)$$

With R being the covariance matrix of measurement noise and Q being the covariance matrix of process noise:

$$Q = \begin{bmatrix} 0 & 0 & 0 \\ 0 & \delta_w & 0 \\ 0 & 0 & \delta_{drift} \end{bmatrix} \quad (T13)$$

And

$$R = \begin{bmatrix} \delta_c & 0 \\ 0 & \delta_a \end{bmatrix} \quad (T14)$$

Then by inspecting the sensor signals, the following values are used in the experiments presented in this project:

$$\delta_w = 1 \times 10^{-1}, \delta_{drift} = 1 \times 10^{-6},$$

$$\delta_c = 1 \times 10^{-5} \text{ and } \delta_a = 5 \times 10^{-2}$$

These values indicate that the gyrometer measurement is more reliable than that of the accelerometer and that the

gyrometer's drift is relatively small when compared to the dynamics producing the angular velocity.

VI. SIMULATION RESULTS

A. PD controller results assuming measuring the tilt angle of the nonlinear model

The simulation results of the nonlinear model of STEVE on flat road with rotation using PD controller gains ($K_p = 600$, $K_d = 350$) is shown in figure 9 and figure 10. If the rider rotates the throttle grip that fixed on the handlebar then rotation commands are given to the vehicle. The rider specifies the needed rotation velocity by the rotation angle of the throttle grip. In the case shown in figure 9 the rider gives a rotation commands to rotate the vehicle to the right with rotation velocity equal $5^\circ/\text{sec}$ for 5 seconds. The vehicle rotates approximately with the specified rotation velocity and the rotation angle changed from 0° to 25° and that seems to be good results.

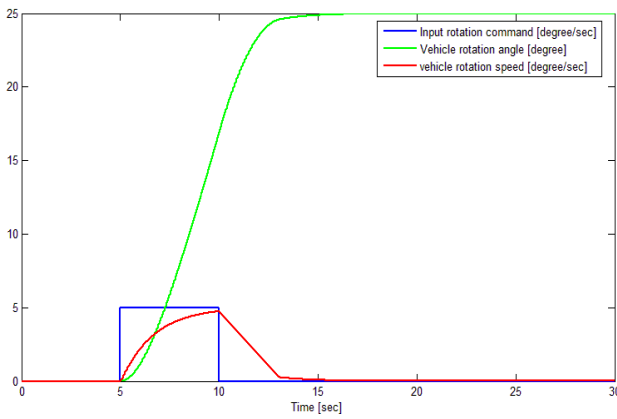


Figure 9. The response of the system for the rotation command.

In the case of figure 10 the rider produced an input torque of 15N.m for 9seconds, and then the tilt angle of the rider is changed from 0° to 2° . When the rider stops his commands the tilt angle of the rider returns to zero. As a result of this human command the speed of the vehicle is changed from 0m/sec to 1.8m/sec and when the rider stops his commands the speed became constant. Also as a result of this commands the tilt angle of the platform is changed but it still within $\pm 2^\circ$. These results seem to be good.

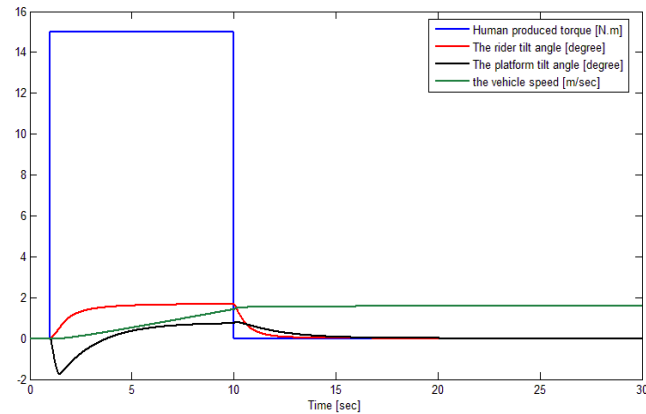


Figure 10. The response of the system for the acceleration commands.

B. Kalman filter results

The simulation results of Kalman filter are shown in figure 11. This is a response for the human produced torque that shown the previous figures which is a realistic case. This results shows that Kalman filter gives a good estimation of the tilt angle. The estimated tilt angle by Kalman filter is approximately has zero error.

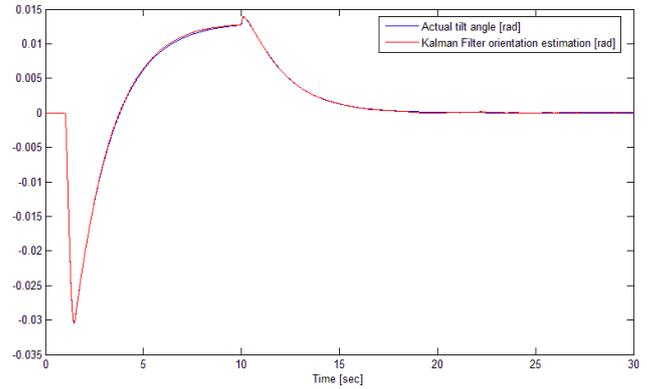


Figure 11. The simulation results of Kalman filter.

C. PD controller results using estimated tilt angle of the nonlinear model

Since Kalman filter make an exact estimation for the tilt angle then the response is the same when using Kalman filter estimation as feedback of the tilt angle for the PD controller. Figure 12 shows the simulation results of the nonlinear model of STEVE on horizontal flat road using Kalman filter as orientation estimation for the feedback.

In the case of figure 12 the rider produced an input torque of -11 Nm for 12 seconds, and then the tilt angle of the rider is changed from 0° to -2.5° . When the rider stops his commands the tilt angle of the rider returns to zero. As a result of this human command the speed of the vehicle is changed from 0 m/sec to -3 m/sec and when the rider stops his commands the speed became constant. Also as a result of this commands the tilt angle of the platform is changed but it still within $\pm 2^\circ$. These results seem to be good.

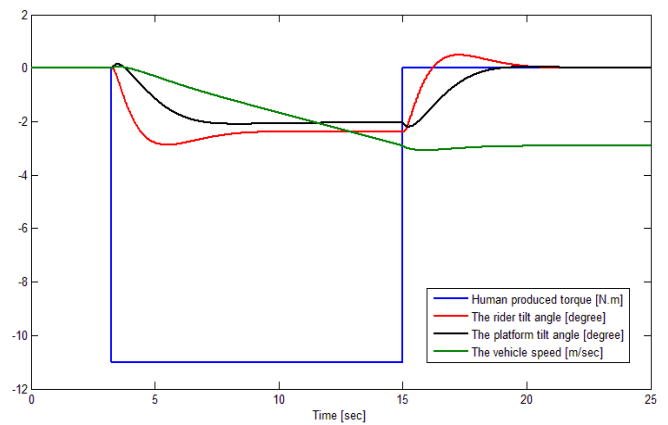


Figure 12. PD controller results using estimated tilt angle of the nonlinear model.

VII. EXPERIMENTAL RESULTS

A. Experimental results of Kalman filter

The calibration of gyrometer and accelerometer is done on the experimental device that shown in figure 13 using XPC target toolbox in MATLAB. It has a built-in encoder in order to give an actual value of the tilt angle. Figure 14 shows the experimental results of the Kalman filter where the error signal is the difference between the actual tilt angle that obtained from the encoder and the estimated tilt angle by Kalman filter. The error is within 2 degree and it seems to be acceptable for the system.



Figure 13. The sensors calibration experiments.

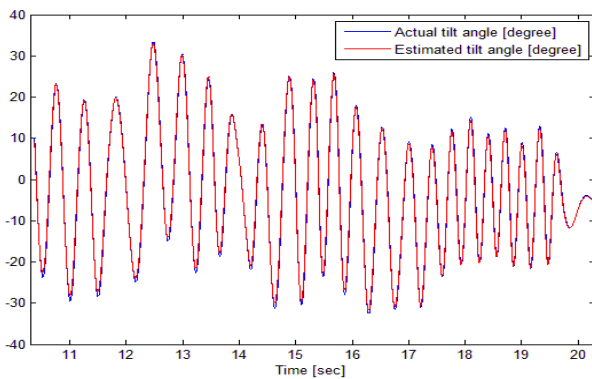


Figure 14. Kalman filter experimental results.

B. Experimental results on the vehicle

To make sure that the embedded control system works correctly hardware-in-the-loop experiments are done to test the controller. Figure 15 shows the hardware-in-the-loop results for the same human produced torque in figure 10.

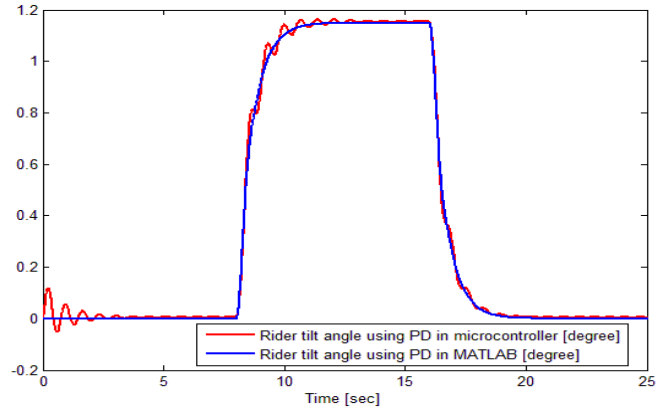


Figure 15. Hardware-in-the-loop experimental results.

VIII. CONCLUSION

In STEVE the control algorithm is implemented through a microcontroller which is the main task of the microcontroller. The microcontroller is one of the major components that are used in this project. The signal from the gyrometer is fused with the accelerometer signal using Kalman filter and accurate angle estimation is obtained

REFERENCES

- [1] Wikipedia, the free encyclopedia, Segway, available at: http://en.wikipedia.org/wiki/Segway_PT
- [2] A. Abuzer, H. Tartory, Self-Balancing Unicycle System on Rough Road, Bachelor Thesis, Palestine Polytechnic University.
- [3] C. Marion, The Segway: Theory, 2006, available at: http://www.chrismarion.net/index.php?option=com_content&view=article&id=122:the-segway-theory&catid=44:robotics&Itemid=240
- [4] Baerveldt, A and Klang, A low-cost and low-weight attitude estimation system for an autonomous helicopter, IEEE international conference on intelligent engineering systems, proceedings, Budapest, Hungary, pp. 391-395.
- [5] K. Tahboub, Biologically - Inspired Humanoid Postural Control, Neurological University Clinic, Neurocenter, University of Freiburg.